Journal of Stress Analysis
Vol. 6, No. 2, Autumn – Winter 2021-22, 21-29
Bu-Ali Sina University

ORIGINAL RESEARCH PAPER

Resistance Spot Welding Process of AISI 304 Steel: Application of Sensitivity Analysis and ANFIS-GWO Methods

M. Safari*, A.H. Rabiee, V. Tahmasbi
Department of Mechanical Engineering, Arak University of Technology, Arak, Iran.

Article info

Article history:
Received 16 November 2021
Received in revised form
10 January 2022
Accepted 25 January 2022

Keywords:
Resistance spot welding
Adaptive neural-fuzzy inference system
Gray wolf optimization algorithm
Sobol sensitivity analysis method
AISI 304 steel

Abstract

For the Resistance Spot Welding (RSW) process, the effects of Welding Current (WC), Electrode Force (EF), Welding Cycle (WCY), and Cooling Cycle (CCY) on the Tensile-Shear Strength (TSS) of the joints have been experimentally investigated. An Adaptive Neural-Fuzzy Inference System (ANFIS) based on data taken from the test results were developed for modelling and predicting of TSS of welds. Optimal parameters of ANFIS system were extracted by Gray Wolf Optimization (GWO) algorithm. The results show that ANFIS network can successfully predict the TSS of RSW welded joints. It can be concluded that the coefficient of determination and mean absolute percentage error for the test section data is 0.97 and 2.45% respectively, which indicates the high accuracy of the final model in approximating the desired outputs of the process. After modeling with ANFIS-GWO, the effect of each input parameter on TSS of the joints was quantitatively measured using Sobol sensitivity analysis method. The results show that increasing in WC, WCY, EF, and CCY leads to an increase in TSS of joints.

Nomenclature

ANFIS	Adaptive neural-fuzzy inference system	ANN	Artificial neural network
ANOVA	Analysis of variance	CCY	Cooling cycle (cycle)
EF	Electrode force (N)	GWO	Gray wolf optimization algorithm
MAPE	Mean absolute percentage error	MAE	Mean absolute error
RMSE	Root mean square error	RSW	Spot welding
WC	Welding current (KA)	WCY	Welding cycle (cycle)
J	Fit function	k	Iteration number
$k_{\max}$	Maximum repetition	O_A	Measured output value
$\overline{O}_A$	Mean of measured output value	O_P	Approximated output value
$\overline{O}_P$	Mean of the approximated output value	ρ^*	Finest solution
P	Solutions vector	V	Updated solution vector
R	First search vector constant	R^2	Coefficient of determination
r	Constant in the search process	S	Coefficient of determination
s	Elements of second search vector constant	q	Uniform distribution of a random number

*Corresponding author: M. Safari (Associate Professor)
E-mail address: m.safari@arakut.ac.ir
http://dx.doi.org/10.22084/jrstan.2022.25065.1195
ISSN: 2588-2597

1. Introduction

RSW is used for joining metallic sheets via fusion of spots at their interfaces. In RSW, two sheet metals are pressed by EF. Then, a WC is applied to the electrodes and therefore, a heat energy is generated between the sheet metals due to their electrical resistance. The key parameter for integrity of the structures fabricated by RSW especially in load-bearing conditions is the mechanical strength of the joints. The RSW is widely employed in manufacturing of sheet metal assembles and stainless steels can be successfully joined with this process. In the case of high-volume productions such as fabrication of car bodies, the RSW is the best welding option due to its high capability in automation for high speed and adaptive production. Regardless of the mentioned advantages of RSW, incompatibility in the welding quality from weld to weld is the big problem of RSW and this reduces the performance of this welding method and increases the costs of fabrication in the automation. Therefore, control of parameters affecting the quality of welding has been one of the important topics of research in the RSW conducted in recent years. Muthu [1] optimized the process parameters in the RSW of AISI 316 stainless steel using Taguchi method. They used the analysis of variance (ANOVA) to find the parameters that influenced the quality of the joints. They obtained that the EF was the most significant parameter in controlling the joints strength. Tavakoli Hoseini et al. [2] investigated the RSW of Inconel alloy 625 with Artificial Neural Network (ANN). They proved that the WC had the greatest effect on the strength of joints while the WCY had the least effect. In addition, they concluded that the ANN was a useful tool for prediction of TSS of RSW welded joints. Kumar et al. [3] studied the effects of parameters on mechanical properties and micro-hardness of stainless steel 304 welded joints. It was concluded that WCY had a significant effect on the TSS. Huang et al. [4] applied an external magnetic field to RSW and concluded that the weld nugget became more regular with less defects. Furthermore, with magnetic field, the TSS of Joints increased. Chen et al. [5] designed a new electrode to reduce the unfavorable interfacial fracture mode. Their results showed that by the proposed electrode, the range of WC that leads to the pullout failure mode is doubled. Karthikeyan and Balasubramaian [6] studied the prediction of TSS load in RSW of aluminum alloy AA2024-T3 using RSM. They optimized the RSW joints and compared the TSS load of welded sheets with friction stir spot welding process. Zhao et al. [7] optimized the RSW with entropy weight method. In their method, the nugget diameter and TSS were converted to a welding quality index. Their results showed that the WC and WCY are the most important parameters affecting the weld quality, respectively. Vignesh et al. [8] investigated the dissimilar RSW of AISI 316 and 2205 Duplex Stainless Steel (DSS) alloys and predicted the effects of parameters on strength of welded joints using experimental tests and numerical simulations. Their results showed that the hardness of heat affected zone for AISI 316 and 2205 DSS is lower and higher compared to the base metal, respectively. Moreover, the fractography results after tensile-shear test proved that the failure occurs in the ductile mode. Xia et al. [9], by calculating the percentage of ejected metal from the melt during the expulsion, evaluated the expulsion intensity in a RSW process. They concluded that the rapid decreasing in signals of force and displacement showed the amount of expelled metal in RSW. Dhawale and Ronge [10] investigated the RSW process of multi spot lap shear specimen. They studied the effects of RSW parameters on the TSS of welded joints. They employed the design of experiments based on Taguchi method and Particle Swarm Optimization (PSO) method to investigate the effect of each process parameter on the strength of joints. Additionally, they optimized the RSW parameters in order to maximize the TSS of the joints. Atashparva and Hamedi [11] investigated the small scale RSW of Nickel based superalloys numerically using COMSOL package. They verified the results of numerical simulations with experimental tests and studied the effects of RSW parameters on TSS and dimensions of weld nugget using the DOE method. Their results proved that the nugget diameter was increased with an increase in WCY and WC and also a decrease in EF. The results of metallography demonstrated the presence of widmanstatten platelets at the weld zone. Ordoñez et al. [12] studied the micro-hardness, TSS and fatigue behavior of RSW joints for DP980 steel sheets and concluded that the stress concentration near the fusion zone leads to a decrease in fatigue life of the welds. Wan et al. [13] compared Back Propagation Neural Network (BPNN) and Probabilistic Neural Network (PNN) for predicting the weld quality in small scale RSW. The results indicated that in estimation of failure load and quality level classification, the BPNN and PNN methods were more proper, respectively. Artificial Intelligence (AI) is widely used to detect the relationship between input and output parameters extracted from a dynamic resistance signal compared to mathematical modeling. Artificial Neural Network (ANN) is used to find the correlation between input and output parameters and is more practical than traditional techniques [14]. ANFIS is a mixture of fuzzy systems and artificial neural network which utilize the learning ability of artificial neural network to attain the fuzzy system parameters [15].

In this paper, ANFIS was utilized to model the influence of main parameters in RSW of AISI 304 steel sheets for predicting of TSS. After that, with the obtained results from ANFIS, the sensitivity of TSS to

variations in each of the input was investigated.

2. Material and Method

2.1. ANFIS

The ANFIS model is a combination of fuzzy inference system and artificial neural network. Merging the fuzzy-set theory and neural network can present advantages and prevail the disadvantages in both methods. The ANFIS has the benefit of having both linguistic and numerical knowledge. The ANFIS model also utilized the neural network ability to identify patterns and classify data. Moreover, other advantages of the ANFIS include its nonlinear ability, adaptation capability, and rapid learning capacity. On the other hand, the main limitation of ANFIS is to obtain the optimal parameters in the model, which should utilize an appropriate optimization algorithm. Fuzzy logic and neural network are used in ANFIS. ANFIS consists of two parts, the antecedent and the sequential, which are interconnected through a set of if-then rules.

2.2. GWO

The GWO was inspired by Canadian Gray Wolf hunting actions by Mirjalili et al. [16]. It has been suggested that they fall into the category of population-based optimization algorithms. Gray wolves have a leading social hierarchy, as revealed in Fig. 1. The pioneers of the crowd are a male and a female known as alpha. The next layer in the gray wolf hierarchy is beta. Beta ones are secondary wolves that aid with alpha in decisions or other group actions. Delta wolf must report to Alpha and Beta, but dominates Omega. Omega has the lowest rank, which should always be obeyed by other wolves.

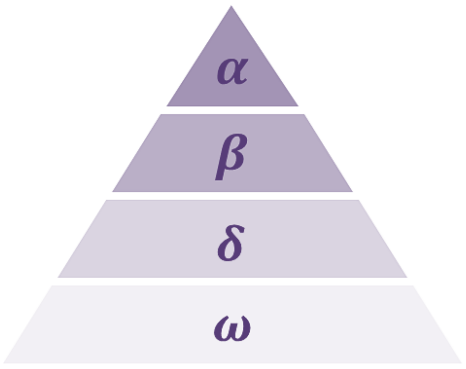

Fig. 1. The hierarchy of gray wolfs.

The GWO algorithm, like the Particle Swarm Optimization algorithm, starts from a random population. In each iteration, the alpha, beta, and delta crowd renew their location according to their prey location. This update also endures until the space among the wolves and the prey is stopped or a satisfactory result is achieved. In GWO, alpha wolves are the finest result. Other crowd tracks along with its dominion. Hunting action is done mainly by alpha and beta wolves and henceforth by the delta followed by omega. Specifically, the GWO consists of the following steps:

Step one: The initial population of gray wolves is randomly created. The created crowd is characterized by the n-dimensional search space for operating M locations. To repeat, start with $k = 0$ initialization and continue to $k_{\max}$.

$$P_j(k) = [P_j^1(k) \dots P_j^f(k) \dots P_j^n(k)]^T, \quad j \in \{\alpha, \beta, \delta\} \tag{1}$$

where $k = 1, 2, \dots, k_{\max}$ are the present iteration numbers, $k_{\max}$ is the maximum repetition, and $P_\alpha(k), P_\beta(k), P_\delta(k)$ is the solutions vector.

Step two: The performance of every single member of the population is assessed based on the accuracy of the approximation of the experimental data of the present problem. Evaluating the performance of each member leads to the value of the fit function (objective function) that is used for the GWO optimization algorithm using: $P_i(k) = \rho,\ i = 1, 2, \dots, M$.

Step three: The finest 3 solutions obtained so far, we mean $P_\alpha(k), P_\beta(k), P_\delta(k)$, are identified by:

$$J(P_\alpha(k)) = \min_{i=j,\dots,M} \{J(P_i(k)), P_i(k) \in D_p\}, \tag{2}$$

$$J(P_\beta(k)) = \min_{i=j,\dots,M} \{J(P_i(k)), P_i(k) \in D_p / P_\alpha(k)\}, \tag{3}$$

$$J(P_\delta(k)) = \min_{i=j,\dots,M} \{J(P_i(k)), P_i(k) \in D_p / P_\alpha(k), P_\beta(k)\}, \tag{4}$$

Eq. (5) has one situation for the outcome:

$$J(P_\alpha(k)) < J(P_\beta(k)) < J(P_\delta(k)) \tag{5}$$

Step four: Search vector constants are obtained utilizing Eqs. (6) and (7):

$$R_j(k) = [r_j^1(k) \dots r_j^f(k) \dots r_j^n(k)]^T \tag{6}$$

$$S_j(k) = [s_j^1(k) \dots s_j^f(k) \dots s_j^n(k)]^T, \quad j \in \{\alpha, \beta, \delta\}, \tag{7}$$

in which:

$$r_j^f(k) = r^f(k)(2q^f - 1), \tag{8}$$

$$s_j^f(k) = 2q^f, \quad j \in \{\alpha, \beta, \delta\}, \tag{9}$$

where q^f the uniform distribution of a random number in the range $0 \le q^f \le 1,\ f = 1 \dots n$ and the constant $r^f(k)$ in the search process is reduced from 2 to 0.

$$r^f(k) = 2[1 - (k-1)/(k_{\max} - 1)], \quad f = 1 \dots n \tag{10}$$

Step five: Search constants factors are permitted to discover their new location by X equations.

$$V_j^i(k) = \left| S_j^f(k) P_j^f(k) - P_i^f(k) \right|, \quad i = 1 \dots M, \quad j \in \{\alpha, \beta, \delta\} \tag{11}$$

By utilization of notation $P^j(k)$ for renewed Alpha, Beta and Delta solutions:

$$P^j(k) = [p^{j1}(k) \dots p^{if}(k) \dots x^{jm}(k)]^T, \quad j \in \{\alpha, \beta, \delta\} \tag{12}$$

The components of these solutions are as follows:

$$P^{if}(k) = p_j^f(k) - r_j^f(k) v_j^i(k), \quad f = 1 \dots n, \quad i = 1 \dots M, \quad j \in \{\alpha, \beta, \delta\}. \tag{13}$$

And the renewed solution vector $P_i(k+1)$ is calculated by Equation X:

$$P_i(k+1) = (P^\alpha(k) + P^\beta(k) + P^\delta(k))/3, \quad i = 1 \dots M. \tag{14}$$

Step six: The updated solution $P_i(k+1)$ is validated by the objective function.
Step seven: The GWO is recurrent from step two till the repetition k reaches the maximum value from the initial value.
Step eight: In the last level, the algorithm stops and the finest solution ever found is saved as:

$$\rho^* = \arg \min_{i=1\dots M} J(P_i(k_{\max})) \tag{15}$$

In Fig. 2, the procedure of eight steps of GWO algorithm is presented in a flowchart.

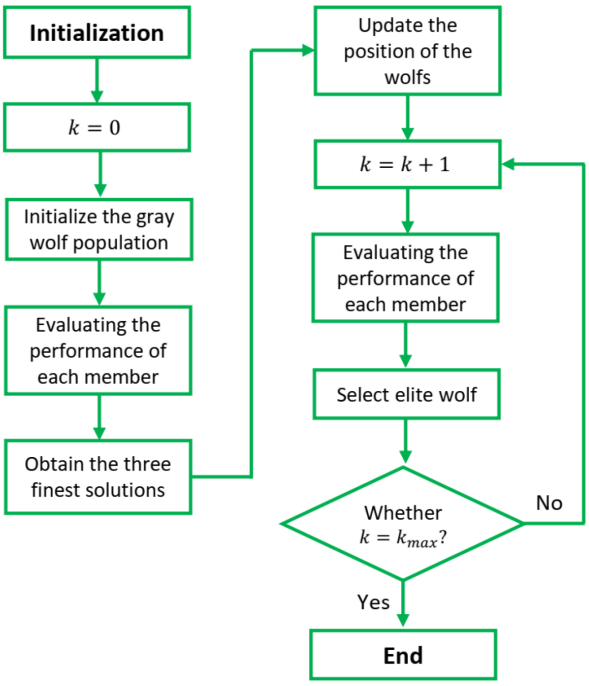

Fig. 2. The flowchart of GWO algorithm.

2.3. Sensitivity Analysis

Sensitivity analysis is a good tool for estimating of the systems and extracting the effect of the input parameters on output for engineering problems which describes the output uncertainty of the model [17]. In addition, the Sobol sensitivity analysis is a powerful method that accurately, quantitatively, and by considering the simultaneous changes of all parameters provides the sensitivity of the output response to changes in input factors in all intervals of the tests.

2.4. Resistance Spot Welding Process

For performing the RSW experiments, a 150 KVA Messer Griesheim machine was used. During the entire period of experiments, the water was circulating in the electrodes in order to improve the heat transfer. AISI 304 steel sheets with thickness = 1mm were used in the RSW experiments. The sheets for RSW experiments had dimensions of length = 150mm, width = 25mm and thickness = 1mm with overlaps of 30mm. Some trial experiments were done for determining the limits of process parameters. The lower limits of the parameters were determined based on the minimum values required to create a suitable joint with sufficient strength, while the upper limits of the parameters were determined based on the creation of a suitable joint without weld expulsion and also excessive reduction of the weld cross section. There are 31 designed experiments based on RSM and Table 1.

Table 1
The limits of RSW parameters.

Parameter	Limits				
WC (KA)	3.6	6.4	9.2	12	14.8
WCY (cycle)	20	25	30	35	40
CCY (cycle)	0	12.5	25	37.5	50
EF (N)	200	800	1400	2000	2600

In Table 2, the performed experiments are presented.

In Fig. 3, a tensile-shear test with Kpruf instrument is shown.

Fig. 3. Tensile-shear test of resistance spot welded AISI 304 sheets.

Some of the joints after tensile-shear test are shown in Fig. 4.

Table 2
The designed RSW experiments based on RSM.

Sample	Welding current (KA)	WCY	CCY	EF (N)
1	6.4	25	12.5	800
2	12.0	25	12.5	800
3	6.4	25	12.5	2000
4	12.0	25	12.5	2000
5	6.4	35	12.5	800
6	12.0	35	12.5	800
7	6.4	35	12.5	2000
8	12.0	35	12.5	2000
9	6.4	25	37.5	800
10	12.0	25	37.5	800
11	6.4	25	37.5	2000
12	12.0	25	37.5	2000
13	6.4	35	37.5	800
14	12.0	35	37.5	800
15	6.4	35	37.5	2000
16	12.0	35	37.5	2000
17	3.6	30	25	1400
18	14.8	30	25	1400
19	9.2	30	25	200
20	9.2	30	25	2600
21	9.2	20	25	1400
22	9.2	40	25	1400
23	9.2	30	0	1400
24	9.2	30	50	1400
25	9.2	30	25	1400
26	9.2	30	25	1400
27	9.2	30	25	1400
28	9.2	30	25	1400
29	9.2	30	25	1400
30	9.2	30	25	1400
31	9.2	30	25	1400

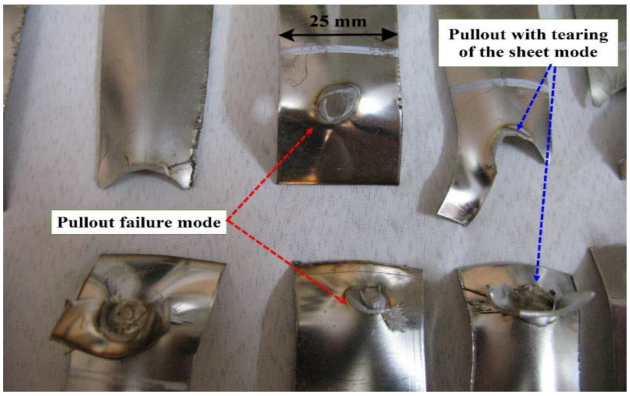

Fig. 4. Some of the RSW joints after tensile-shear test with different failure modes.

As seen in Fig. 4, pullout and pullout with tearing of the sheets modes were observed in the RSW joints. It should be noted that, in order to ensure the repeatability of the tests and increase the accuracy of the measurements, all resistance spot welding tests were repeated three times and the average of tensile-shear strengths was considered as the tensile-shear strength for each test. Furthermore, in order to eliminate random errors, experiments were performed randomly.

2.5. Analysis of Variance (ANOVA)

In Table 3, the ANOVA results for TSS of the joints such as effects of welding parameters and their interactions are presented.

In the ANOVA analysis of engineering problems, the parameters with p-values less than 0.05 are effective inputs [18]. Accordingly, all of process parameters and some of their interactions influence the TSS. Considering $R-sq = 93.30\%$ and $R-sq(adj) = 90.87\%$ for TSS shows the passable accuracy of the suggested model.

Table 3
ANOVA for TSS of AISI 304 steel joints after RSW process.

Source	DF	Adj SS	Adj MS	F-value	P-value
Model	8	58004167	7250521	38.31	0.000
Linear	4	27231667	6807917	35.97	0.000
WC (KA)	1	14260417	14260417	75.35	0.000
WCY	1	1083750	1083750	5.73	0.026
CCY	1	1353750	1353750	7.15	0.014
EF (N)	1	10533750	10533750	55.66	0.000
2-Way Interaction	4	30772500	7693125	40.65	0.000
WC (KA)*WCY	1	12425625	12425625	65.65	0.000
WC (KA)*EF (N)	1	1155625	1155625	6.11	0.022
WCY*EF (N)	1	15015625	15015625	79.34	0.000
CCY*EF (N)	1	2175625	2175625	11.50	0.003
Error	22	4163808	189264		
Lack-of-Fit	16	4094665	255917	22.21	0.001
Pure Error	6	69143	11524		
Total	30	62167974			

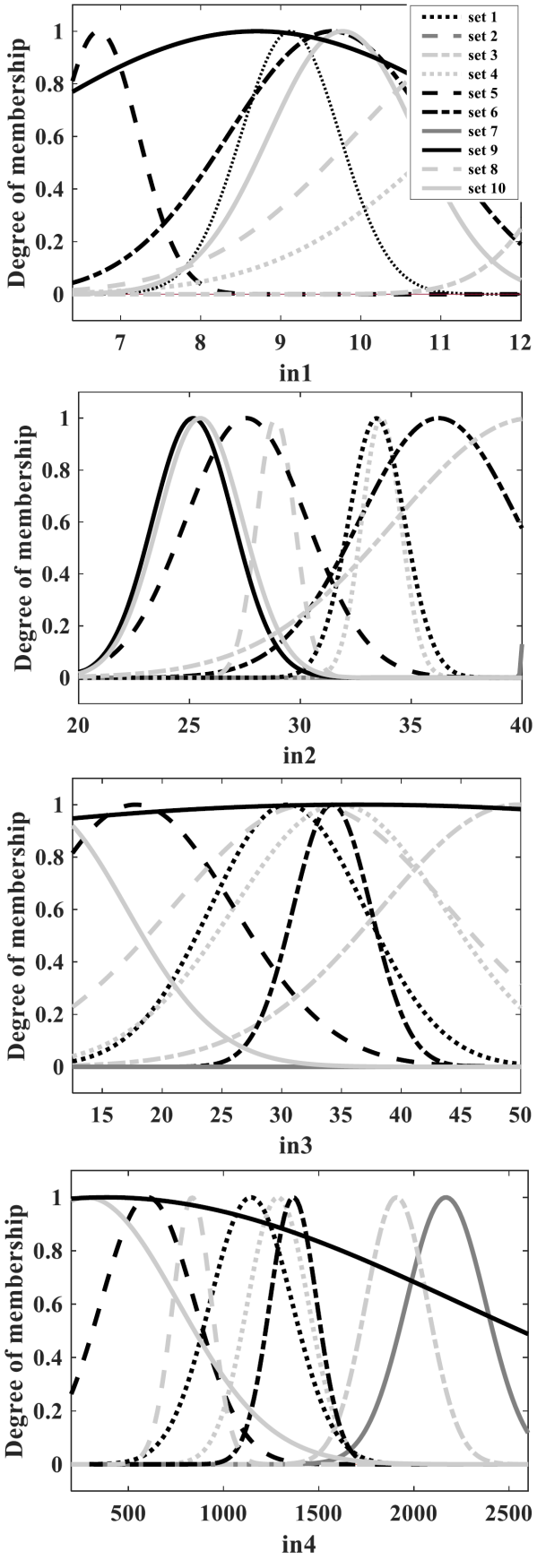

Fig. 5. The optimized membership function for WC (in1), WCY (in2), CCY (in3) and EF (in4).

3. Results and Discussion

3.1. The Results of ANFIS-GWO System

In the present study, there are 31 empirical data for ANFIS construction, involving four inputs and single output (TSS). This data collection is arbitrarily separated into 2 subsets, 70% for training and 30% for testing. Fig. 5 shows the optimized Gaussian membership functions associated with WC, WCY, CCY and EF, respectively.

Moreover, Fig. 6 shows the actual experimental data and also predicted data attained by ANFIS for both the training and testing phases. The accuracy of the ANFIS predicted data is very high for the training section as long as the ANFIS is trained based on the data of this section. Next, Fig. 7 shows the value of the TSS of welded joints for the actual and predicted data in both the training and testing sections. As can be seen in these diagrams, the actual experimental data and ANFIS predicted data in the training phase coincide quite well. The second part of the diagrams (test section) also show that the ANFIS is able to predict the data related to the test section. Moreover, Fig. 8 illustrates the error histogram for both training and testing phases. It can be seen here that the error frequency is greater at values closer to zero especially for training part.

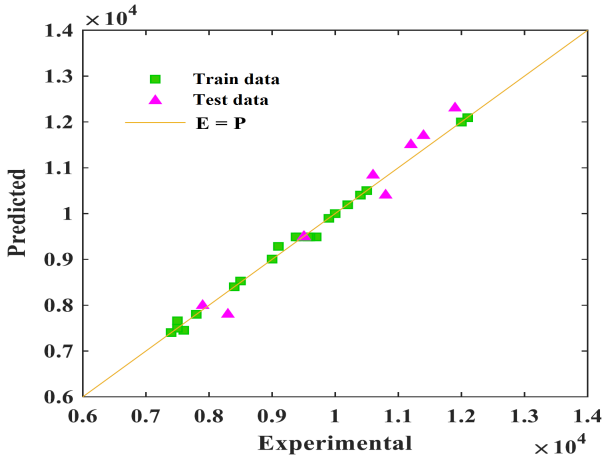

Fig. 6. Comparison between experimental and predicted data.

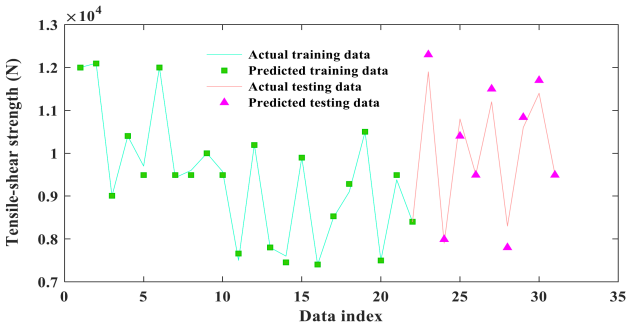

Fig. 7. Differences between experimental and test data for prediction of TSS.

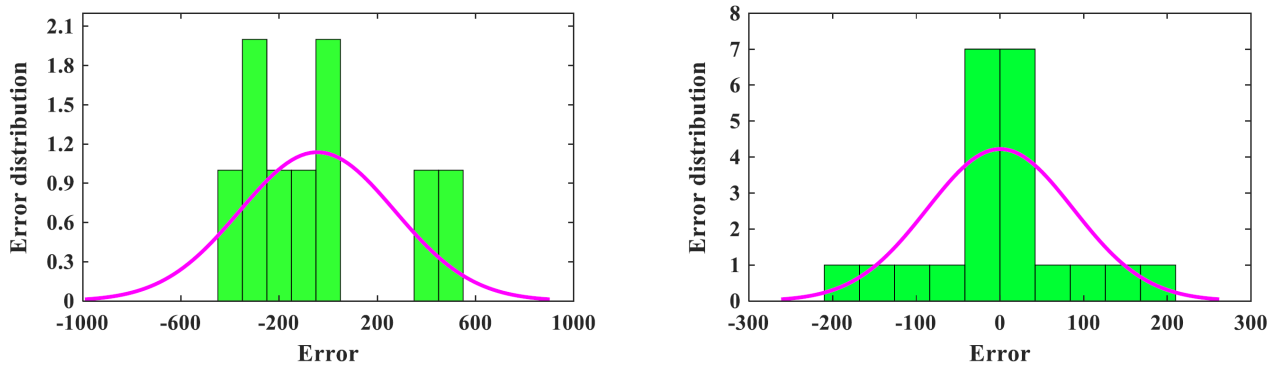

Fig. 8. Error histogram for training and texting sections.

Moreover, Fig. 9 demonstrates the normalized error associated with the training and testing sections. As can be seen, the amount of error in the test section is greater than that of the training section.

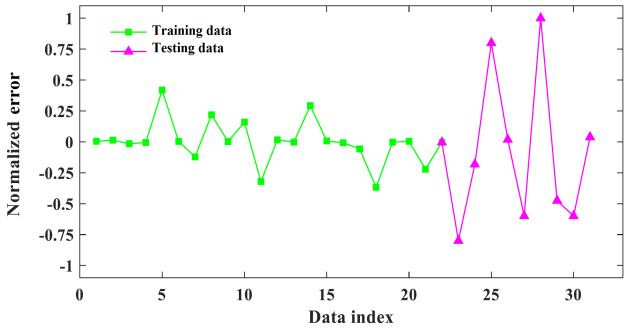

Fig. 9. Normalized error for the training and testing sections.

In addition, for quantitative analysis of the developed model, various statistical criteria such as Mean Absolute Error (MAE), Root Mean Square Error (RMSE), coefficient of determination (R^2 or R-squared), and Mean Absolute Percentage Error (MAPE) were used.

$$\mathrm{RMSE} = \sqrt{\frac{1}{n}\sum_{i=1}^{n}\left(O_A - O_P\right)^2} \tag{16}$$

$$\mathrm{MAE} = \frac{1}{n}\sum_{i=1}^{n}\left|O_A - O_P\right| \tag{17}$$

$$R^2 = \frac{\left[\sum_{i=1}^{n}\left(O_A - \overline{O}_A\right)\left(O_P - \overline{O}_P\right)\right]^2}{\left[\sum_{i=1}^{n}\left(O_A - \overline{O}_A\right)\right]\left[\sum_{i=1}^{n}\left(O_P - \overline{O}_P\right)\right]} \tag{18}$$

$$\mathrm{MAPE} = \frac{100\%}{n}\sum_{i=1}^{n}\left|\frac{O_A - O_P}{O_A}\right| \tag{19}$$

where O_A is the measured output value for the i-th data, O_P is the approximated output by the ANFIS for the i-th sample, $\overline{O}_A$ is the mean of measured data and $\overline{O}_P$ is the mean of the predicted data. To examine the model accuracy, the above-mentioned criteria are independently computed for training and test sections, as shown in Table 4.

From the listed values in Table 4, it proves that the ANFIS is a powerful tool for prediction of TSS. The criteria RMSE and MAE are small, while they alone are not appropriate for model evaluation. Next, R^2 and MAPE criteria that determine the amount of error relative to the number of data are used. The coefficient of determination, R^2, is so close to one, indicating the high accuracy of the model. The percentage errors of MAPE in the training section are 0.58%. Furthermore, the MAPE in the test section are 2.54%. It can be seen here that the calculated error in some cases (in the test section) is relatively larger, because the test data have not been used in model training and recognize as unseen data. However, the mean absolute error for the test section is in reasonable range, which indicates high accuracy of the obtained model. Thus, due to the existence of error in empirical data, this amount of error in estimation is to be expected.

Table 4
RMSE, MAE, R^2 and MAPE criteria for TSS of welded joints.

	RMSE	MAE	R^2	MAPE (%)
Train	85	51	0.99	0.58
Test	301	251	0.97	2.54

3.2. The Effects of RSW Input Parameters on TSS Based on Sensitivity Analysis

Figs. 10 and 11 show the increase in TSS with increasing the WC and WCY because of increase in the heat generation in welding zone and accordingly the penetration depth. In addition, the TSS of the joints can improve with an increase in EF (Fig. 12). The reason is that with increasing the EF, the indentation of the electrodes in the sheets increases and excessively increasing in the EF leads to decrease in the cross-section of the welded joints. Therefore, the strength of RSW joint decreases with an increase in the EF. However, it is proved from Fig. 13 that increasing the CCY leads to increase in TSS because of solidifying the weld metal before liberation the welded specimens and this leads to increase in the joint strength.

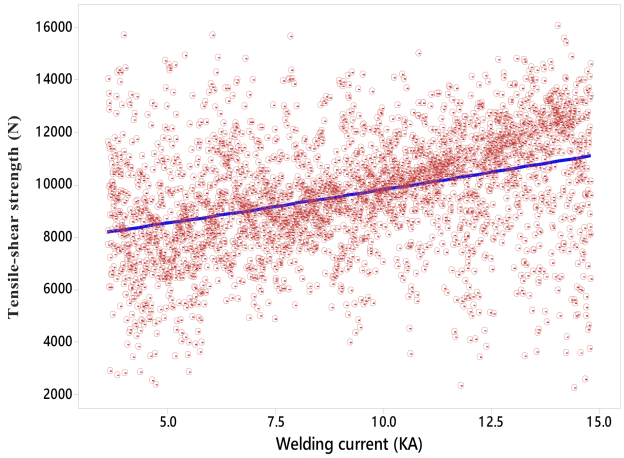

Fig. 10. Effect of WC on TSS of the joints.

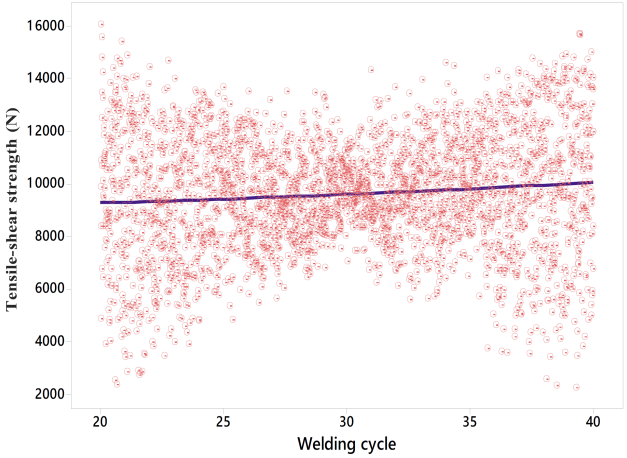

Fig. 11. Effect of WCY on TSS of the joints.

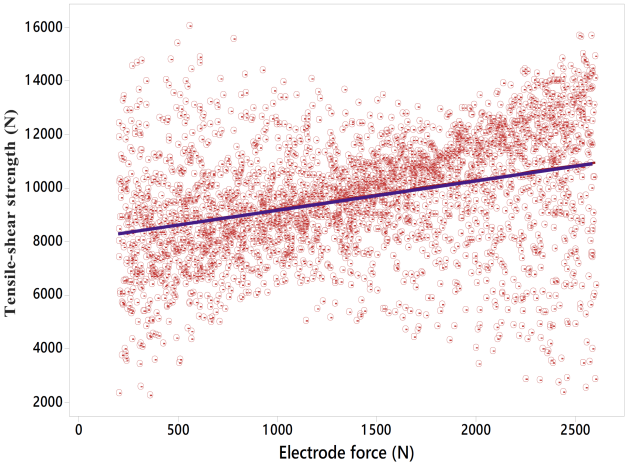

Fig. 12. Effect of EF on TSS of the joints.

Fig. 14 shows the result of Sobol sensitivity analysis for the TSS obtained by Simlab software. It is seen from Fig. 14, the WCY, WC, EF, and CCY have the greatest effect on the strength of the joints, respectively.

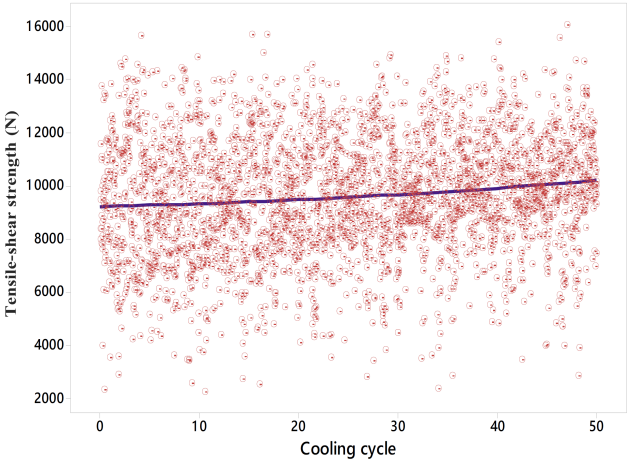

Fig. 13. Effect of CCY on TSS of the joints.

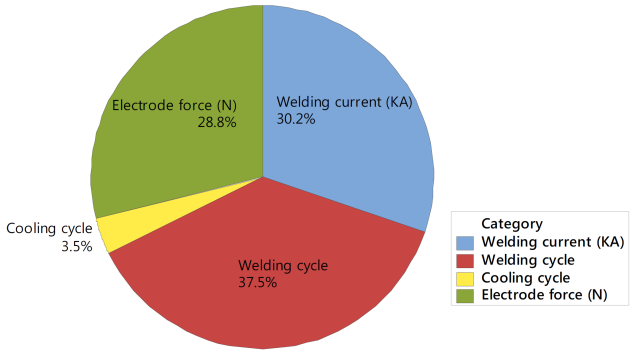

Fig. 14. The diagram of effectiveness of input parameters on TSS of RSW joints.

4. Conclusions

RSW process of AISI 304 steel sheets was experimentally studied by investigation of the effects RSW parameters on the strength of the joints using ANFIS (based on GWO) and Sobol sensitivity method. Following results were obtained:

1. It was concluded that the TSS increased with increasing the WC and WCY because of the increase in the heat generation of welding zone and accordingly the penetration depth. In addition, the TSS of the joints can improve with an increase in EF. The reason is that with increasing the EF, the indentation of the electrodes in the sheets increased and excessively increasing in the EF led to decrease in the cross-section of the welded joints. However, it was proved that increasing the CCY led to increase in TSS because of solidifying the weld metal before liberation the welded specimens.

2. The ANFIS results showed that the employed network is a powerful tool for prediction of TSS based on variable input variables.

3. The results of Sobol sensitivity analysis showed that the WCY, WC, EF, and CCY have the greatest effect on the strength of the joints, respectively.

References

[1] P. Muthu, Optimization of the process parameters of resistance spot welding of AISI 316l sheets using Taguchi method, Mech. Mech. Eng., 23(1) (2019) 64-69.

[2] H. Tavakoli Hoseini, M. Farahani, M. Sohrabian, Process analysis of resistance spot welding on the Inconel alloy 625 using artificial neural networks, Int. J. Manuf. Res., 12(4) (2017) 444-460.

[3] R. Kumar, J.S. Chohan, R. Goyal, P. Chauhan, Impact of process parameters of resistance spot welding on mechanical properties and micro hardness of stainless steel 304 weldments, Int. J. Struct. Integrity, 12(3) (2021) 366-377.

[4] M. Huang, Q. Zhang, L. Qi, L. Deng, Y. Li, Effect of external magnetic field on resistance spot welding of aluminum alloy AA6061-T6, J. Manuf. Processes, 50 (2020) 456-466.

[5] T. Chen, Z. Ling, M. Wang, L. Kong, Effect of a slightly concave electrode on resistance spot welding of Q&P1180 steel, J. Mater. Process. Technol., 285 (2020) 116797.

[6] R. Karthikeyan, V. Balasubramaian, Optimization of electrical resistance spot welding and comparison with friction stir spot welding of AA2024-T3 aluminum alloy joints, Mater. Today: Proc., 4(2) (2017) 1762-1771.

[7] D. Zhao, M. Ivanov, Y. Wang, D. Liang, W. Du, Multi-objective optimization of the resistance spot welding process using a hybrid approach, J. Intell. Manuf., 32 (2021) 2219-2234.

[8] K. Vignesh, A. Elaya Perumal, P. Velmurugan, Resistance spot welding of AISI-316L SS and 2205 DSS for predicting parametric influences on weld strength-experimental and FEM approach, Arch. Civ. Mech. Eng., 19(4) (2019) 1029-1042.

[9] Y.J. Xia, Z.W. Su, Y.B. Li, L. Zhou, Y. Shen, Online quantitative evaluation of expulsion in resistance spot welding, J. Manuf. Processes, 46 (2019) 34-43.

[10] P.A. Dhawale, B.P. Ronge, Parametric optimization of resistance spot welding for multi spot welded lap shear specimen to predict weld strength, Mater. Today: Proc., 19 (2019) 700-707.

[11] M. Atashparva, M. Hamedi, Investigating mechanical properties of small scale resistance spot welding of a nickel based super lloy through statistical DOE, Exp. Tech., 42(1) (2018) 27-43.

[12] J.H. Ordoñez, R.R. Ambriz, C. García, G. Plascencia, D. Jaramillo, Overloading effect on the fatigue strength in resistance spot welding joints of a DP980 steel, Int. J. Fatigue, 121 (2019) 163-171.

[13] X. Wan, Y. Wang, D. Zhao, Y. Huang, A comparison of two types of neural network for weld quality prediction in small scale resistance spot welding, Mech. Syst. Sig. Process., 93 (2017) 634-644.

[14] Y. Cho, S. Rhee, Quality estimation of resistance spot welding by using pattern recognition with neural networks, IEEE Trans. Instrum. Meas., 53(2) (2004) 330-334.

[15] B.N. Panda, M.R. Babhubalendruni, B.B. Biswal, D.S. Rajput, editors. Application of artificial intelligence methods to spot welding of commercial aluminum sheets (B.S. 1050). K.N. Das et al. (eds.), Proceedings of Fourth International Conference on Soft Computing for Problem Solving, Advances in Intelligent Systems and Computing, Springer India, (2015) 335.

[16] S. Mirjalili, S.M. Mirjalili, A. Lewis, Grey wolf optimizer, Adv. Eng. Software, 69 (2014) 46-61.

[17] I.M. Sobol, Sensitivity analysis for non-linear mathematical models, Math. Modelling. Comput. Experiments, 4 (1993) 407-414.

[18] D.C. Montgomery, Design and Analysis of Experiments, John Wiley & Sons Publisher, (2017).